Mechanism of the slow-moving landslides in Jurassic red-strata in the Three Gorges Reservoir, China

Haibo Miao[a, c], Gonghui Wang[b, *], Kunlong Yin[a], Toshitaka Kamai[b], Yuanyao Li[c]

Abstract:

Landslides in Jurassic red-strata make up a great part of geohazards in the Three Gorges Reservoir (TGR) in China. Most of them begin to move slowly with the accumulated displacement increasing stepwise, which corresponds to seasonal rainfall and 30 meters of reservoir water level fluctuation (145 m to 175 m on elevation). We analyzed the movement of 21 slow moving landslides in Jurassic red-strata in TGR, and found that all these landslides involved in two differing processes; one is the sliding process with different shear speeds of soils within the sliding zone (landslide activity), and the other one is in steady state with different durations (dormant state). This means that the soil within the sliding surface may experience shearing at different shear rates and recovery in shear strength during the dormant period. To clarify the mechanism of this kind of movement, we took soil samples from the sliding surface of Xiangshanlu landslide, which occurred on August 30, 2008 in Jurassic red-strata in TGR, and examined the shear rate dependency and recovery of shear resistance by means of ring shear tests. The results of tests at different shear rates show that the shear strength is positively dependent on the shear rate, and can be recovered within short consolidation duration after the shearing ceased. By increasing the pore-water pressure (PWP) from the upper layer of the sample, we also examined the

initiation of shearing which can simulate the restart of landsliding due to the fluctuation of groundwater level caused by rainfall or changes in reservoir water level. The monitored PWP near the sliding surface revealed that there was delayed response of PWP near the sliding surface to the applied one. This kind of delayed response in pore-water pressure may provide help for the prediction of landslide occurrence due to rainfall or fluctuation of reservoir water level.

Keywords: landslides; the Three Gorges Reservoir; Jurassic red-strata; slow movement; shear resistance; shear rate effect

1. Introduction

The Three Gorges Reservoir in China (hereinafter we call TGR, its location is shown in Fig. 1) is an area with a large number of landslides (Chen, 1999; Deng et al., 2000; Wu et al., 2001; Li, 2002; Liu, et al., 2004; Wen et al., 2007; Jian et al., 2009; Li et al., 2013, among others). These landslides developed in all strata, especially in Jurassic stratum. The Jurassic lithology in TGR is continental lake facies sedimentary rocks, the colors of which are mainly fuchsia, maroon, or red brown; therefore, the Jurassic stratum is often called "red-strata" by Chinese academe (Li et al., 2002; Chen et al., 2004; Xu et al, 2010). From the lithology structure of Jurassic red-strata in TGR, the interbedding layer of thick silty-sandstone and thin sandy-mudstone is an important reason for the development of weak bands with high content of clay mineral like montmorillonite and illite in the long geological history (Jian et al., 2005, 2008), which caused some typical landslides, such as Chonggang landslide (Yin et al., 1993), four landslide groups in Wanzhou area (Jian et al., 2009), Jipazi landslide (Huang, 2007), Qianjiangping landslide (Wang, et al., 2004; Liao et al, 2005) and so on. It has been reported that among the landslides selected in the second and the third phase of mitigating and monitoring projects in TGR supported by Chinese government, more than 70% are in Jurassic red-strata (Chai et al., 2009). Up to now, many studies had been performed on the landslides occurring in Jurassic red-strata in the TGR area with focus on examining the geological basis (say, possible clay mineral in the weak bands of potential sliding surface). However, the mechanism of the movement in the

pre-failure stage, especially in the case of slow movement of landslides influenced by seasonal rainfall and periodic reservoir water level fluctuation, is not yet well understood.

In this paper, we investigate the movements of 21 landslides in the Jurassic red-strata in TGR and examined the moving types of these landslides. The ring shear apparatus developed by Disaster Prevention Research Institute, Kyoto University, was used to simulate the shear process of the soils within the sliding zone in the slow movement through the case study of a landslide occurred on August 30, 2008, in Jurassic red-strata in TGR. We performed three groups of tests, i.e., test with different shear rates, test with different consolidation duration and, tests with changing the pore-water pressure of shear band. Based on the results, three aspects such as shear rate effect, recovery of residual shear strength and trigger of landslide reactivation, are discussed to reveal the mechanism of the slow movement of the landslides in Jurassic red-strata in the Three Gorges Reservoir.

2 Type of the slow movement

To reduce the risk from landslides in TGR, Chinese government approved many projects which involve systematic investigation of landslides and potentially unstable slopes, ancient landslides reactivation and their failure mechanism, especially the monitoring of large landslides (Wen et al., 2007). In many cases the surface monitoring data are much easier to be obtained through using a wide range of techniques such as survey markers, extensometers, and digital photogrammetry, as well as global position system (GPS) and interferometric synthetic aperture radar (InSAR). As a result, in the monitoring of these large landslides in

72 TGR, GPS measurements which can provide the surface displacements have been widely
73 used. Petley et al. (2002, 2005) demonstrated that the patterns of landslide movement provide
74 an insight into the processes occurring in the sliding zone, and used the surface monitoring
75 data to interpret landslide movement patterns, which mainly includes four types: (1) very slow
76 or creep movement, which occurs at the moment of formation of the tension area located on
77 the crown or flanks of the landslide; (2) low velocity movements, caused by gradual
78 formation of the shear surface; (3) rapid movement because of the sliding mass
79 disaggregating into loose materials; (4) very rapid movement as a result of landside fails.
80 In this study 21 landslides monitored by GPS in Jurassic red-strata in TGR were
81 examined. In each landslide, 2-9 GPS stations were installed according to its scale. We
82 obtained the accumulated displacements of monitoring points from January 2007 to
83 November 2009 (35 months). We studied the monitoring point with the largest accumulated
84 displacement for each landslide, and plotted 21 curves as showed in Fig. 2. These curves can
85 be divided into two groups (Figs. 2a, b) according to the displacements. In Fig. 2a, 15 curves
86 of accumulated displacement versus time display “random oscillation” or “trending
87 oscillation” with an average sliding rate < 6 cm/year. These oscillations in the accumulated
88 displacement might result from the measurement errors that are normally intensive in the tiny
89 data range (Ueno et al., 2003). Other 6 landslides (Fig. 2b) had their displacements increased
90 mainly stepwise with their sliding rates greater than 6 cm/year but smaller than 1.5 m/year.
91 For the first group, all the landslides were in very slow movement or creep movement, which
92 could be classified as the first style of the movement of rotational and translational landslides

as described by Petley et al. (2005). However, for the second group the six landslides showed slow movement according to the sliding rate proposed by Schuster & Krizek (1978). Because all GPS stations in each landslide were installed soon after cracks occurred in the walls of houses locating on the slope, following the interpretation by Petley et al. (2005), we inferred that the movement shown in Fig. 2a mainly resulted from the crack propagation (shear surface generation), whereas the slow movement (Fig. 2b) resulted from the occurrence of movement along existing sliding surface..

Irrespective of the differences in the accumulated displacement, all the displacements showing slow movement (Fig. 2b) increased stepwise, which can by conceptually illustrated by a model shown in Fig. 3a. Differentiating this stepwise displacement gives an increasing or decreasing displacement rate, indicating that the landslide would experience alternations of accelerating and decelerating movements (Fig. 3b). Therefore, it is expected that the soils within the sliding zone would undergo two processes; one is shearing at differing shear rates, and the other one is recovery of shear strength under a constant normal stress with different duration. These two processes correspond to the sliding and dormant periods, respectively. Therefore, in order to understand the mechanism of the slow-moving landslides in Jurassic red-strata in TGR, two questions should be answered: (1) how does the landslide come into reactivation from dormant state as shown conceptually in Fig. 3; (2) how does the movement stop and keep staying at the dormant state?

3 Ring shear test

3.1 Testing sample

To reveal the mechanism of these slowly moving landslides in Jurassic red-strata in the TGR, we took soil samples along the sliding surface from Xiangshanlu landslide, which occurred in the early morning on August 30, 2008. This landslide is located on the left bank of Tongguluo River, a tributary of the Yangtze River in Shazhenxi Town, Zigui country in TGR (Fig. 4). The landslide covers an area of 3.3×10^4 m^2 and has a volume of 0.165×10^6 m^3. The sliding mass was composed of Quaternary colluvium and eluvium, and the lithology of sliding bed rock is middle Jurassic Qianfoyan Formation (J_2q), as well as the soils along the sliding surface are silty clay with the thickness of 10 cm, formed by weathering of mudstone and sandy-mudstone (Fig. 5). It is noted that we also took samples from boring cores taken from differing landslides shown in Fig. 2b, but the volumes of the cores near the sliding surface were not enough for the performance of ring shear tests. We compared the physical properties (see, Table 1) of these core samples to those of Xiangshanlu landslide, and found that they are basically the same. Therefore, in the following we only conducted ring shear tests on the samples taken from Xiangshanlu landslide as an example.

The testing sample is remolded from soils within the sliding zone, which mainly consists of silt (about 92%) with 30% clay. The grain size distribution of the sample is presented in Fig. 6a. Some physical property indexes such as dry density, liquid limit, plastic limit, plasticity index and uniformity coefficient, as well as the coefficient of curvature, are listed in Table 1. The plasticity chart is showed in Fig. 6b. In result, the testing sample (hereinafter we call this sample as XSL) is low liquid limit silty clay.

3.2 Ring shear apparatus

Ring shear apparatus has been widely used in examining the shear behavior of the soil with large shear displacement and the residual shear strength for the analysis of slope stability (Bishop et al., 1971; Bromhead, 1979; Hungr and Morgenstern, 1984; Stark and Contreras, 1996; Wang and Sassa, 2002; Sassa et al., 2004; Wang et al., 2007, 2010; Sadrekarimi and Olson, 2009). The ring shear apparatus used in the present research is DPRI-4 with the shear area of 314.16 cm^2, which was developed in Disaster Prevention Research Institute at Kyoto University, Japan (Sassa et al., 2004). This apparatus enables the simulation of many different kinds of static and dynamic loading under drained or undrained conditions. The samples can be sheared by means of torque-controlled or shear speed-controlled method (Wang and Sassa, 2002; Sassa et al., 2003).

3.3 Testing procedure

The testing procedure consisted of three parts: sample preparation, consolidation and shearing. During the sample preparation, distilled water was firstly added to the oven dried sample to elevate the initial water content close to its plastic limit, and then the sample was stirred evenly. After keeping the sample for 72 hours in a sealed container to ensure the uniform distribution of moisture, the sample was placed into the shear box. After the placement of the sample and the set-up of shear system, we measured the friction between the upper pair of rings and the rubber edges at the adjusted gap value for the employed ring shear

apparatus. This measured friction was then subtracted from the measured shear resistance to obtain the real shear strength of the sample (Sassa et al., 2003, 2004).

After the measurement of friction of rubber edges, the sample was normally consolidated under a normal stress of 98 kPa without applying any shear stress. It is noted that we planned to shear the sample at differing normal stress levels. However, here, we used 98 kPa as the first normal stress level, just because the ring shear apparatus was designed for tests under higher normal stress (up to 2 MPa), and servo control system does not enable better performance if the applied normal stress is too small, say, less than 50 kPa.

After consolidation under the normal stress of 98 kPa was finished (evidenced by no further change in sample volume), we sheared the sample drained at a shear rate of 0.0011 mm/s to measure the residual shear strength. Using the same method, we measured the residual shear strength at three differing normal stress levels (98, 147, and 196 kPa). We also examined the shear rate dependency of residual shear strength by shearing the same sample at differing shear rates while keeping the normal stress constant (196 kPa). We further examined the effect of consolidation duration on the strength recovery. After the shear test with the normal stress of 196 kPa was finished, the sample was kept in consolidation with the same normal stress, for 1 day, 3 days, 5 days and 17 days, respectively. At the end of each consolidation process, the sample was sheared with the same shear rate under the same normal stress. Finally, after the above mentioned tests were finished, we consolidated the sample for 14 days under the normal stress of 196 kPa and shear stress of 40 kPa (corresponding to a slope angle of 11.5 degrees), and then applied a pore-water pressure of 80

kPa from the upper drainage tube to check the possible response of pore water pressure within the shear zone.

4 Testing results

4.1 Basic shear behavior of tested soils

The shear behavior and residual shear strength of XSL sample were obtained. Figure 7a shows the normal stress, shear resistance and pore-water pressure (PWP) against the shear displacement for the test under the normal stress of 98 kPa. At the beginning of shearing (the shear displacement < 4 mm), the PWP increased almost linearly with shear displacement, thereafter it decreased slowly with progress of shearing, and the shear resistance increased correspondingly. Because this test was performed under drained condition, we inferred that the monitored PWP resulted from the unbalance between the generation and dissipation rates of PWP. In the first shearing stage (say within 4 mm of shear displacement), PWP generation rate might be greater than the dissipation rate due to the reduction in porosity of soil layers near the sliding surface. This would result in the buildup of excess PWP. It is noted that a vertical displacement of about 0.3 mm was observed within the first 4 mm of shear displacement (called dilation, see, Pudasaini and Hutter, 2007). With further progress of shearing, PWP generation rate would become smaller than the dissipation rate, and then the excess PWP would become smaller.

The residual shear strengths obtained under three differing normal stresses are plotted in Fig. 7b against the effective normal stresses. The line (residual failure line) bonding these

three points has a y-intercept of 18 kPa and a slope angle of 13 degrees. According to the Mohr-Coulomb criterion, the effective residual cohesion of the tested sample is 18 kPa and the effective residual internal friction angle is 13 degrees.

4.2 Shear rate effect

According to the movement features summarized in Fig. 2, these landslides in Jurassic red-strata in TGR have different moving speeds in different active stage. This means that the soil layer within the shear zone may suffer from differing rates of shearing. To clarify the possible effects of shear rates on the shear behavior and then on the landsliding, we sheared the sample to residual state at different shear rates under drained condition, and in each test we kept the normal stress constant (196 kPa).

We performed multistage testing, which has been found to produce results similar to testing of individual samples (Bromhead, 1992; Tika et al., 1996; Harris and Watson, 1997; Tiwari and Marui, 2004; Suzuki et al., 2004). At first, we sheared the sample at a displacement rate of 0.001135 mm/s (the lowest rate available by the ring shear apparatus employed in this study) to the residual state, and then elevated the rate to a differing one to measure the residual shear strength at this new shear rate. With the same test process, we sheared the sample at 13 different displacement rates.

The results of the tests performed at different shear rates are presented in Fig. 8 which plots the shear resistance at each shear displacement rate. As shown in Fig. 8, the shear resistance became greater with increase of shear displacement rate, and the fitted curve of all

219 the data points presents a growth-oriented power function. The residual shear resistance at the
220 shear displacement rate of 175.56 mm/s (115.4 kPa) was approximately twice that obtained at
221 the shear displacement rate of 0.0011 mm/s (58.2 kPa), indicating that the shear strength is
222 strongly dependent on the shear displacement rate.
223
224 **4.3 Recovery of shear strength with consolidation period**
225 When landslides reach the dormant state, the shear strength could be recovered (Gibo et
226 al., 2002; Nakamura, 2002; Carrubba & Del Fabbro, 2008), and it is expected that the
227 recovered shear strength is time dependent. As shown in Fig. 2, these landslides experienced
228 the dormant state with different periods. Therefore, it is expected that the shear strength
229 would be recovered in some extent. In order to understand the recovery of shear strength of
230 soils within sliding zone after different consolidation durations, we performed ring shear test
231 on the sample with different consolidation durations.
232 Acknowledging that the residual shear strength of clayey soils has no association with the
233 initial structure and stress history of the soil (Mitchell, 1976), after the tests using differing
234 shear displacement rates, we kept the soil sample in consolidation for 1 day, 3 days, 5 days
235 and 17 days respectively under the normal stress of 196 kPa (hereinafter, we call them as test
236 TC1, TC3, TC5 and TC17, respectively). At the end of each consolidation process we sheared
237 the sample at the same shear displacement rate of 0.0077 mm/s.
238 The measured shear resistance and vertical displacement are plotted in Figs. 9a, b,
239 respectively, against the shear displacement. From Fig. 9a, we find that the peak shear

strengths obtained from TC5 was greater than that of TC3 and also both of them were greater than that of TC1. This indicates that the shear strength could be recovered with consolidation period. However, with further increase of the consolidation period, the recovery in the peak shear strength is small, which can be seen from the test results from TC17. It is also noted that the shear strengths at the shear displacement of 250 mm were different for these four tests, probably due to volume change in the sample with progress of shearing. It has been clarified that a shear zone will be formed and become thicker with progress of shearing (shear included dilation, see, e.g., Pudasaini and Hutter, 2007) in ring shear tests on sandy soils (Wang and Sassa, 2002; Wang et al., 2007; Wang et al., 2010). If the sandy soils were in loose state after the consolidation, the shear zone will become denser. This is evidenced by the monitored vertical displacement shown in Fig. 9b, where the vertical displacement became a bit greater with progress of shear time. Re-shearing the denser shear zone will result in greater peak shear strength, but should not result in any difference in the residual shear strength. Therefore, we inferred that these differences in the shear strength at the shear displacement of 250 mm resulted from the fact that the shear did not reach the real residual shear state yet. From Fig. 9a, we conclude that the shear strength could be recovered in short period, say less than 5 days. Considering the main purpose of these tests is examining the possible strength regain through comparing the peak shear strength, here we won't make further discussion on the relationship between the formation of shear zone and residual shear strength.

4.4 Response of pore-water pressure within the shear band

As well known, reservoir landslide is normally influenced by periodic fluctuation of reservoir water level and/or seasonal rainfall. Groundwater table or pore-water pressure within the soil layers of the landslide will be changed due to the fluctuation of reservoir water level and/or precipitation. This kind of change will result in the decrease of effective normal stress that causes the decrease of shear strength of soils within the sliding zone. To examine the possible response of pore-water pressure of the soils near the sliding surface in the field to this kind of variation of reservoir water level or groundwater table, we performed ring shear test to examine the possible response of pore water pressure near the shear zone of specimen to the change of pore-water pressure outside of the specimen.

After the above-mentioned test TC17 was finished, we changed the shear model from shear-speed control to shear-stress control one. Using this shear-stress control model, we consolidated the sample under a stress state with the normal stress being 196 kPa and shear stress being 40 kPa. After the consolidation, we applied a water pressure of 80 kPa from the upper part of the specimen by using another ring shear apparatus through a plastic pipe (Fig. 10). As shown in Fig. 10b, firstly we put the water into shear box of the left ring shear apparatus and then applied a normal stress of 80 kPa on the water. The applied water pressure will load soon on the upper part of the sample in the ring shear box.

The monitored pore water pressure near the shear band (sliding surface) is plotted in Fig. 11a together with the applied normal stress, applied shear stress, shear displacement, and effective normal stress. It is seen that the pore water pressure gradually elevated. Dissipating of water pressure from the top of the sample to the shear band took approximately 6,000

seconds. Thereafter, the pore-water pressure started to increase gradually. Figure 11b presents the effective stress path together with the residual shear strength envelop (RSSE). With the increasing of pore-water pressure near the shear band, the effective normal stress gradually moved leftward to the RSSE. However, this moving process took a long time, because of the small initial applied stress (40 kPa), and also probably due to the lower permeability of the sample. About 95,000 seconds later (26 hours and 40 minutes), we increased the shear stress artificially loaded on the shear band from 40 kPa to 70 kPa, and then shear failure occurred with a continuously increased shear displacement (after point 'Failure', marked with an ellipse in Fig. 11b). According to Fig. 11b, it is expected that if the shear stress was increased to 54 kPa, shear failure would be triggered. However, after 14 days of consolidation the residual shear strength of the sample had a certain recovery (about 16 kPa). As the result, a shear stress greater than the residual shear strength will be needed to trigger the shear failure or reactivate the landsliding.

In addition, from this ring shear test we found a delayed response of pore water pressure within the soil layer near the sliding surface to the applied pore pressure. This delayed response follows the principle of pressure diffusion in soils, which has been used to study the rainfall-induced landslides (Haneberg, 1991; Reid, 1994), reservoir-induced seismicity (Talwani and Acree, 1984) and also landslide movement triggered by atmospheric tides (Schulz et al., 2009a).

For the landslide triggered by rainfall and/or reservoir water level fluctuation, the variable pore pressure will be applied on the sliding mass above the shear surface. In this condition,

303 the diffusion of the pore pressure will occur, and then result in the change of pore water
304 pressure in the shear band. However, this change in the shear band will take a certain time
305 that is determined by the hydraulic diffusivity of the soils of sliding mass above the shear
306 band. In other words, there will be a delayed response of landsliding to rainfall and/or
307 fluctuation of reservoir water level.
308
309 **5. Discussion**
310 **5.1 Shear speed effect and residual shear strength recovery**
311 The effect of shear speed on the shear behavior of natural soils is complex. Lupini
312 (1980) and Lupini et al. (1981) firstly investigated the influence of shear speed on the
313 residual shear strength. Martins (1982), Skempton (1985), Lemos et al. (1985), Lemos
314 (1986), Tika (1989), and Tika et al. (1996) carried out further studies to examine the effect
315 of shear rate on the residual shear strength of differing types of soils.
316 Skempton (1985) showed that in slow shearing at the rate within 0.01 mm/min, the
317 variation of shear rate had tiny effect on the residual shear strength, while for the shear rate
318 larger than 100 mm/min the effect was significant, which was related to clay fraction of the
319 soils. Lemos et al. (1985) proposed three types of variation of the residual strength with an
320 increasing rate of displacement, i.e. positive, neutral, and negative rate effect. Lupini (1981)
321 recognized three modes of residual shearing of cohesive soils, which is turbulent mode,
322 transitional mode and sliding mode. The mechanism was confirmed as proportions of platy

particles to rotund particles present in the soil and the coefficient of inter particle friction of the platy particles. The similar conclusions were also summarized by Tika et al. (1996).

According to Fig. 8, the role of positive shear rate effect on the residual shear strength in the slow movement of landslides in Jurassic red-strata in the TGR can be explained as follows. Firstly, when the landslide is trigged, the displacement rate increases because of the initial positive acceleration. Secondly, due to the positive shear rate effect, the residual shear strength becomes greater. As a result, the displacement rate increases to a maximum value until the positive acceleration reduces to zero. Thirdly, when the residual shear resistance at the maximum shear speed is larger than sliding force, deceleration appears which results in the decrease in displacement rate with the reduction in residual shear strength. Finally the deceleration reduces to zero and the landslide movement stops.

From the movement features summarized in Fig. 2b and the conceptual model illustrated in Fig. 3, it is expected that the landslide would enter into a dormant state after a certain period of decelerating movement. It is well known that for a landslide with pre-existing shear zone, the shear strength of the soils within the sliding zone will be in residual state when the landslide is in dormant stage, and will gain a certain recovery when the landslide enters the dormant state (Ren et al., 1996; Gibo et al., 2002; Nakamura, 2002). As shown in Fig. 9, the residual shear strength of the tested sample revealed a fast recovery, indicating that once the landslide entered the dormant state, shear resistance increased and then additional force (such as rainfall, earthquake, etc.) would be necessary to reactivate the landslide.

344

345 **5.2 Landslide reactivation**

346 It has been reported that soil saturation due to the fast infiltration of rainfall is the main
347 reason for the initiation of a huge number of shallow landslides (De Vita et al., 1998; Pasuto
348 and Silvano, 1998; Polemio and Sdao, 1999; Hilley et al., 2004; Coe et al., 2004; Aleotti,
349 2004). For the landslides in reservoir area, fluctuation of the water level plays a key role in
350 the initiation of instability of embankment slopes due to the change in water content and
351 seepage conditions in the slope (Schuster, 1979; Pudasaini and Miller, 2012b). This can be
352 exemplified by the Vaiont landslide in Italy (Genevois and Ghirotti, 2005), and also by the
353 Qianjiangping landslide in the Three Gorges Reservoir (Wang et al., 2004).

354 For a landslide in the reservoir, the pore-water pressure of soils within the sliding zone
355 changes following seasonal rainfall and periodic water level fluctuation, indicating the rise
356 and fall of the underground water table respectively. The monitoring data of tensiometer
357 and GPS has shown that dormant landslides in the Three Gorges Reservoir accelerated as
358 the underground water rose and decelerated as it fell (Wang et al., 2008; Yin et al, 2010).
359 These conditions can be explained by using Mohr-Coulomb failure rule and Newton's
360 second law of motion (Schulz et al, 2009b).

361 The variation of shear resistance of the sliding soil within the shear band can be
362 expressed as $\tau_f(t) = c + \{\sigma - [u_w + p(z,t)]\}\tan\phi$, where $\tau_f(t)$ is the shear resistance of the
363 sliding soil within the shear band, and $p(z,t)$ is the pore pressure at distance z (hear the
364 depth of the sliding mass above the sliding surface), which is the result of pore pressure

365 diffusion due to the application of fluctuating reservoir water level and rainfall (Talwani
366 and Acree, 1984; Haneberg, 1991; Reid, 1994); c and ϕ are the cohesion and internal
367 friction angle of soils within the sliding zone respectively; σ and u_w are the total normal
368 stress and pore-water pressure of the soils within the sliding zone respectively.

369 The above expression for $\tau_f(t)$ says that the changing of pore water pressure of the
370 sliding soil within the shear band will have a delayed time *t*, because the diffusion of
371 pore-water pressure in the landslide depends on the hydraulic conductivity, the thickness of
372 sliding mass and the externally applied load due to the fluctuation of the water level induced
373 by the landslide impact generated water waves in the reservoir (Pudasaini and Miller,
374 2012b). For the reactivation of dormant landslide in Jurassic red-strata in TGR, the soil
375 layer above sliding surface (or sliding mass) are mainly 6 m to 20 m. As a result, the
376 response will be delayed more significantly. This may be the reason why the monitored
377 landslide displacement showed sharp increment often after the heavy rainfall or the water
378 level regulation of TGR.

379 Around 2490 landslides had been identified in the TGR area before the construction of
380 the dam, and great efforts had been paid to manage or monitor some large landslides at high
381 risk. However, more detailed survey since the impoundment of the reservoir revealed that
382 there are more than 5700 landslides (Liu et al., 2009), and many of them are reactivated
383 ones. Due to the financial limitation, engineering countermeasures had been performed only
384 on those landslides at high risk of catastrophic failure, while other dangerous landslides
385 could only be monitored. Therefore, understanding the reactivation and movement

386 mechanisms of those seemingly dormant landslides is of great importance for the mitigation
387 of landslide hazards in TGR area.

388 Cracks on the walls of houses or fissures on the ground on a slope had been normally
389 regarded as the precursors of landslides. However, the appearance of cracks or fissures does
390 not mean that sliding surface has been formed (Kamai, 1998). In this aspect, the monitored
391 displacements summarized in Fig. 2a are consistent with the results obtained in other
392 landslides (e.g., Suemine, 1983; Kamai, 1998; Petley et al., 2002), and may provide help for
393 identifying whether the slope in Jurassic red-strata is at the failure-surface transmission state
394 or has already entered the residual (sliding) state (Kamai, 1998). This is important for the
395 stability analysis because the mobilized shear strengths at differing states will be different.

396 From Fig. 2b, we found that these slow moving landslides in Jurassic red-strata
397 experienced movement with differing velocities. Although this kind of movement may
398 result from many factors, such as rainfall and variation of water level in the reservoir, the
399 variation of residual shear strength of the sample with shear rate may also play a key role in
400 the movement. When the landsliding becomes faster, the shear resistance will become
401 greater to decelerate the movement. Therefore, it is expected that these landslides will
402 experience continuous accelerating-decelerating process, similar to the dynamics of a
403 rainfall-triggered landslide in Japan reported by Wang et al. (2010).

404 It is well known that for the landslides in reservoir area, fluctuation of the water level
405 plays a key role in the initiation of instability of embankment slopes due to the change in
406 water content and seepage conditions in the slope. The change in interstitial fluid pressure is

one of the most important material parameters determining the landslide initiation and the dynamics of the flow and the depositional characteristics. The flow pattern, flow mobility, runout distance, deposition morphology and energy dissipation are substantially influenced by the pore water pressure (Sassa 1988; Iverson and Denlinger, 2001; Pitman and Le, 2005; Pudasaini et al., 2005; Sassa and Wang, 2005; Pudasaini, 2012; Pudasaini and Miller, 2013). On the one hand, this means that the accurate knowledge of the pore fluid pressure is very crucial for the reliable predictions of the flow event and their dynamics. While on the other hand, the data obtained here can be utilized to validate landslide and mass flow models by back simulating the sliding mass, the fluid wave and dam walls interactions, submarine mass flows, their deposition fans and extents (Pudasaini and Miller, 2012b) in technically, geologically and environmentally more sensitive huge man made reservoirs and dams, including the 1963 Vaiont landslide (Genevois and Ghirotti, 2005), and the landslides in TGR in China. The model and unified simulation method proposed by Pudasaini and Miller (2012a, b) can be applied to adequately describe the change (fluctuation) of water level in the reservoir due to landslide impact at the reservoir. This is an important aspect, because it plays a key role in the initiation of instability of embankment slopes due to the change in water content and seepage conditions in the slope.

6. Conclusions

This paper presents the basic movement features of 21 landslides occurring in the Jurassic red-strata in TGR and discusses the landslide's slow moving behavior. Three

groups of ring shear tests were performed to examine the possible mechanisms for different types of landslide movements. Shear speed effect, residual shear strength recovery and landslide reactivation trigger, are discussed to reveal the mechanisms of the slow-moving landslides in Jurassic red-strata in TGR. We draw the following conclusions.

(1) The movement of the landslide in Jurassic red-strata in the TGR before the catastrophic failure can be divided into two differing states, i.e., the slow movement with different sliding rates, and the creep movement due to the crack propagation.

(2) The residual shear strength is positively dependent on the shear rate. This may be one of the main reasons for the decelerating movement resulting in the cease of landsliding. Further, the residual shear strength of the soils within the sliding zone could have a certain recovery in a short time. This will elevate the stability of the landslides in Jurassic red-strata in TGR. This makes the reactivation of the landslide less likely.

(3) The landslides in Jurassic red-strata in TGR display a delayed response to the rainfall and/or periodic fluctuation of reservoir water level. This delay depends on the permeability, the thickness of landsliding mass, and also the externally applied load due to the fluctuation of the water level induced by the landslide impact generated water waves in the reservoir.

Acknowledgements

This study was supported by the National Natural Science Foundation of China (No. 41101515, No. 41202247 and No. 41240023). Also this study was partially supported by

the Fundamental Research Funds for the Central Universities, China University of Geosciences (Wuhan), No. CUGL110203. The authors thank Wei Wang, Xiawei Yi, Jiang Wu and Yingchun Li for the works in the field investigation and sample collecting. The first author would like to thank Dr. Hiroshi Fukuoka, Associate Professor in Disaster Prevention Research Institute, Kyoto University, for his help when the first author was staying in Kyoto University for this joint research. Finally, the authors' special thanks go to the editor and referees of this paper; whose valuable comments led to substantial improvement of this paper.

References

Aleotti, P., 2004. A warning system for rainfall-induced shallow failures. Engineering Geology 73(3-4), 247-265.

Bishop, A.W., Green, G.E., Garga, V.K., Andresen, A., Brown, J.D., 1971. A new ring shear apparatus and its application to the measurement of residual strength. Géotechnique 21(4), 273-328.

Bromhead, E.N., 1979. A simple ring shear apparatus. Ground Engineering 12(5), 40-44.

Bromhead, E.N., 1992. Stability of slopes, 2nd Ed., Surrey University Press, London.

Carrubba, P., Del Fabbro, M., 2008. Laboratory investigation on reactivated residual strength. Journal of Geotechnical and Geoenvironmental Engineering 134(3), 302-315.

Chai, B., Yin, K.L., Jian, W.X., Dai, Y.X., 2009. Analysis of water-rock interaction characteristics and bank slope failure process of red-strata. Journal of Central South University (Science and Technology), 40(4), 1092-1098 (in Chinese).

Chen, D.J., 1999. Engineering geological problems in the Three Gorges Project on the Yangtze, China. Engineering Geology 51(3), 183-193.

Chen, Q., Kou X.B., Huang, S.B., Zhou, Y.J., 2004. The distributes and geologic environment characteristics of red beds in China. Journal of Engineering Geology 12(1), 34-40 (in Chinese).

Coe, J.A., Michael, J.A., Crovelli, R.A., Savage, W.Z., Lappade, W.T., Nashem, W.D., 2004. Probabilistic assessment of precipitation-triggered landslides using historical records of landslide occurrence, Seattle, Washington. Environmental and Engineering Geoscience 10(2), 103-122.

De Vita, P., Reichenbach, P., Bathurst, J.C., Borga, M., Crosta, G., Crozier, M., Glade, T., Guzzetti, F., Hansen, A., Wasowski, J., 1998. Rainfall-triggered landslides: a reference list. Environmental Geology 35(2-3), 219-233.

Deng, Q.L., Zhu, Z.Y., Cui, Z.Q., Wang, X.P., 2000.Mass rock creep and landsliding on the Huangtupo slope in the reservoir area of the Three Gorges Project, Yangtze River, China. Engineering Geology 58(1), 67-83.

Genevois, R., Ghirotti, M., 2005. The 1963 Vaiont landslide. Giornale di Geologia Applicata 1, 41-52.

Gibo, S., Egashira, K., Ohtsubo, M., 2002. Strength recovery from residual states in reactivated landslides. Géotechnique 52(9), 683-686.

Haneberg, W.C., 1991. Pore-pressure diffusion and the hydrologic response of nearly saturated, thin landslide deposits to rainfall. The Journal of Geology 99(6), 886-892.

Harris, A.J., Watson, P.D.J., 1997. Optimal procedure for the ring shear test. Ground Engineering 30(6), 26-28.

Hilley, G.E., Burgmann, R., Ferretti, A., Novali, F., Rocca, F., 2004. Dynamics of slow-moving landslides from permanent scatterer analysis. Science 304, 1952-1955.

Huang, R.H., 2007. Large-scale landslides and their sliding mechanisms in China since the 20th century. Chinese Journal of Rock Mechanics and Engineering 26(3), 434-454 (in Chinese)

Hungr, O., Morgenstern, N.R., 1984. Ring velocity ring shear tests on sand. Géotechnique 34(3), 415-421.

Iverson, R.M., Denlinger, R.P., 2001. Flow of variably fluidized granular masses across three-dimensional terrain: 1. Coulomb mixture theory. Journal of Geophysical Research: Solid Earth (1978-2012), 106(B1): 537-552.

Jian, W.X., Yin, K.L., Ma, C.Q., Liu, L.L., Zhang C., 2005. Characteristics of incompetent beds in Jurassic red clastic rocks in Wanzhou. Rock and Soil Mechanism 26(6), 901-905 (in Chinese).

507 Jian, W.X., Yin, K.L., Luo, C., Yao, L.L., Zhang, C., 2008. Slip zone characteristics of
508 Anlesi landslide in Wanzhou of Three Gorges Reservoir area. Earth science – Journal
509 of China University of Geosciences 33(5), 672-678 (in Chinese).
510 Jian, W.X., Wang, Z.J., Yin, K.L., 2009. Mechanism of the Anlesi landslide in the Three
511 Gorges Reservoir, China. Engineering Geology 108(1-2), 86-95.
512 Kamai, T., 1998. Monitoring the process of ground failure in repeated landslides and
513 associated stability assessments. Engineering Geology 50(1-2), 71-84.
514 Lemos, L.J.L., Skempton, A.W., Vaughan, P.R., 1985. Earthquake loading of shear surfaces
515 in slopes. In proceedings of 11th International Conference on Soil Mechanics and
516 Foundation Engineering, 1955-1958.
517 Lemos, L.J.L., 1986. The effect of rate on residual strength of soil. Ph.D. Thesis, Imperial
518 Collage London (University of London).
519 Li, L.R., 2002. Geological hazards and prevention in the Three Gorges dam area. Land and
520 Resources 4, 4-7.
521 Li, T.Y., Wang, J.L., 2002. Chinese red beds and landforms. Journal of Sichuan Normal
522 University (Natural Science) 25(4), 427-431 (in Chinese).
523 Li, Y.R., Wen, B.P., Aydin, A., Ju, N.P., 2013. Ring shear tests on slip zone soils of three
524 giant landslides in the Three Gorges Project area. Engineering Geology 154, 106-115.
525 Liao, Q.L., Li, X., Li, S.D., Dong Y.H., 2005. Occurrence, geology and geomorphy
526 characteristics and origin of Qiangjiangping landslide in Three Gorges Reservoir area

and study on ancient landslide criterion. Chinese Journal of Rock Mechanics and Engineering 24(17), 3146-3153 (in Chinese).

Liu, C.Z., Liu Y.H., Wen, M.S., Li, T.F., Lian, J.F., Qin, S.W., 2009. Geo-hazard initiation and assessment in the Three Gorges Reservoir. In: Landslide Disaster Mitigation in Three Gorges Reservoir, China (Wang and Li, eds). Springer, pp.3-40.

Liu, J.G., Mason, P.J., Clerici, N., Chen, S., Davis, A., Miao, F., Deng, H., Liang, L., 2004. Landslide hazard assessment in the Three Gorges area of the Yangtze River using ASTER imagery: Zigui‐Badong. Geomorphology 61(1-2), 171‐187.

Lupini, J.F., 1980. The residual strength of soils. Ph.D. Thesis, Imperial Collage London (University of London).

Lupini, J.F., Skinner, A.E., Vaughan, P.R., 1981. The drained residual strength of cohesive soils. Géotechnique 31(2), 181-213.

Martins, J.P., 1982. Shaft resistance of axially loaded piles in clay. Géotechnique 32(4), 369-384.

Mitchell, J.K., 1976. Fundamentals of soil behavior. New York: John Wiley and Sons, Inc.

Nakamura, S., 2002. Studies on residual strength and strength recovery from residual state for landslide soils. Science Bulletin of the Faculty of Agriculture, University of the Ryukyus, 49: 97-142 (in Japanese with English abstract).

Pasuto, A., Silvano, S., 1998. Rainfall as a trigger of shallow mass movements. A case study in the Dolomites, Italy. Environment Geology 35(2-3), 184-189.

547 Petley, D.N., Bulmer, M.H., Murphy, W., 2002. Patterns of movement in rotational and
548 translational landslides. Geology 30(8), 719-722.
549 Petley, D.N., Mantovani, F., Bulmer, M.H., Zannoni, A., 2005. The use of surface
550 monitoring data for the interpretation of landslide movement patterns. Geomorphology
551 66(1-4), 133-147.
552 Pitman, E.B., Le, L., 2005. A two-fluid model for avalanche and debris flows. Philosophical
553 Transactions of the Royal Society A: Mathematical, Physical and Engineering
554 Sciences 363(1832), 1573-1601.
555 Polemio, M., Sdao, F., 1999. The role of rainfall in the landslide hazard: the case of the
556 Avigliano urban area (Southern Apennines, Italy). Engineering Geology 53(3-4),
557 297-309.
558 Pudasaini, S.P., 2012. A general two-phase debris flow model. Journal of Geophysical
559 Research: Earth Surface (2003-2012), 117(F3), doi:10.1029/2011JF002186.
560 Pudasaini, S.P., Wang, Y., Hutter, K., 2005. Modelling debris flows down general channels.
561 Natural Hazards and Earth System Science 5(6), 799-819.
562 Pudasaini, S.P., Hutter, K., 2007. Avalanche dynamics: dynamics of rapid flows of dense
563 granular avalanches, Springer, Berlin, New York.
564 Pudasaini, S.P., Miller, S.A., 2012a. Buoyancy induced mobility in two-phase debris flow.
565 AIP Conference Proceedings-American Institute of Physics, 1479(1): 149-152.
566 Pudasaini, S.P., Miller, S.A., 2012b. A real two-phase submarine debris flow and tsunami.
567 AIP Conference Proceedings-American Institute of Physics, 1479(1): 197-200.

568 Pudasaini, S.P., Miller, S.A., 2013. The hypermobility of huge landslides and avalanches.
569 Engineering Geology, 157: 124-132.
570 Reid, M.E., 1994. A pore-pressure diffusion model for estimating landslide-inducing
571 rainfall. The Journal of Geology 102(6), 709-717.
572 Ren, G.M., Nie, D.X., Zuo, S.S., 1996. Study on cohesion restoration of slide zone soil.
573 Journal of Geological Hazards and Environment Preservation 7(3), 7-12 (in Chinese).
574 Sadrekarimi, A., Olson, S.M., 2009. A new ring shear device to measure the large
575 displacement shearing behavior of sands. ASTM Geotechnical Testing Journal 32(3),
576 197-208.
577 Sassa, K., 1988. Special lecture: the geotechnical model for the motion of landslides.
578 Proceedings of the 5th International Symposium on Landslides, Lausanne, vol.1, 33-52.
579 Sassa, K., Wang, G., Fukuoka, H., 2003. Performing undrained shear tests on saturated
580 sands in a new intelligent type of ring shear apparatus. ASTM Geotechnical Testing
581 Journal, 26(3): 257-265.
582 Sassa, K., Fukuoka, H., Wang, G.H., Ishikaka, N., 2004. Undrained dynamic-loading
583 ring-shear apparatus and its application to landslide dynamics. Landslides, 1(1): 7-19.
584 Sassa, K., Wang, G.H., 2005. Mechanism of landslide-triggered debris flows: Liquefaction
585 phenomena due to the undrained loading of torrent deposits. In Debris-flow hazards
586 and related phenomena (pp. 81-104). Springer Berlin Heidelberg.
587 Schulz, W.H., Kean, J.W., Wang, G.H., 2009a. Landslide movement in southwest Colorado
588 triggered by atmospheric tides. Nature Geoscience 2(12), 863-866.

589 Schulz, W.H., McKenna, J.P., Kibler, J.D., Biavati, G., 2009b. Relations between
590 hydrology and velocity of a continuously landslide – evidence of pore-water pressure
591 feedback regulating landslide motion? Landslides 6(3), 811-190.
592 Schuster, R.L., 1979. Reservoir-induced landslides. Bulletin of the International Association
593 of Engineering Geology 20(1), 8-15.
594 Schuster, R.L., Krizek, R. (Editors), 1979. Landslides: analysis and control. Transportation
595 Research Board, National Academy of Sciences, Washington, D.C., Special Report
596 176, 234pp.
597 Skempton, A.W., 1985. Residual strength of clays in landslides folded strata and the
598 laboratory. Géotechnique 35(1), 1-18.
599 Stark, T.D., Contreras, I.A., 1996. Constant volume ring shear apparatus. ASTM
600 Geotechnical Testing Journal 19(1), 3-11.
601 Suemine, A., 1983. Study on landslide mechanism in the area of crystalline schist (part
602 1)—an example of propagation of Rankine state. Bulletin of the Disaster Prevention
603 Research Institute of Kyoto University 33 (3), 105–127.
604 Suzuki, M., Kobayashi, K., Yamamoto, T., Matsubara, T., Hukuda, J., 2004. Influence of
605 shear rate on residual strength of clay in ring shear test. Research Report, School of
606 Engineering, Yamaguchi University 55(2), 49-62.
607 Talwani, P. and Acree, S., 1984. Pore pressure diffusion and the mechanism of
608 reservoir-induced seismicity. Pure and Applied Geophysics 122(6), 947-965.

609 Tika, T.E., 1989. The effect of fast shearing on the residual strength of soils. Ph.D. Thesis,
610 Imperial Collage London (University of London).
611 Tika, T.E., Vaughan, P.R., Lemos, L.J.L., 1996. Fast shearing of pre-existing shear zone in
612 soil. Géotechnique 42(2), 197-233.
613 Tiwari, B., Marui, H., 2004. Objective oriented multistage ring shear test for shear strength
614 of landslide soil. Journal of Geotechnical and Geoenvironmental Engineering 130(2),
615 217-222.
616 Ueno, M., Itani, K., Langley, R. B., 2003. Real-time GPS landslide monitoring under poor
617 satellite visibility. In Proceedings of 2003 International Symposium on GPS/GNSS,
618 Tokyo, Japan, pp. 15-18.
619 Wang, F.W., Zhang, Y.M., Huo, Z.T., Matsumoto, T., Huang B.L., 2004. The July 14, 2003
620 Qiangjiangping landslide, Three Gorges Resrvoir, China. Landslides 1(2), 157-162.
621 Wang, F.W., Zhang, Y.M., Huo, Z.T., Peng, X.M., Araiba, K., Wang, G.H., 2008. The July
622 14, 2003 Movement of the Shuping landslide in the first four years after the initial
623 impoundment of the Three Gorges Dam Reservoir, China. Landslides 5(3), 321-329.
624 Wang, G.H., Sassa, K., 2002. Post-failure mobility of saturated sands in undrained
625 load-controlled ring shear tests. Canadian Geotechnical Journal 39(4), 821-837.
626 Wang, G.H., Sassa, K., Fukuoka, H., Tada, T., 2007. Experimental study on the shearing
627 behavior of saturated silty soils based on ring-shear tests. Journal of Geotechnical and
628 Geoenvironmental Engineering 133(3), 319-333.

629 Wang, G.H., Suemine, A., Schulz, W.H., 2010. Shear-rate-dependent strength control on
630 the dynamics of rainfall-triggered landslides, Tokushima Prefecture, Japan. Earth
631 Surface Processes and Landforms 35(4), 407-416.
632 Wen, B.P, Aydin, A., Duzgoren-Aydin, N. S., Li, Y.R., Chen, H.Y., Xiao, S.D., 2007.
633 Residual strength of slip zones of large landslides in the Three Gorges area, China.
634 Engineering Geology 93(3-4), 82-98.
635 Wu, S.R., Shi, L., Wang, R.J., Tan, C.X., Hu, D.G., Mei, Y.T., Xu R.C., 2001. Zonation of
636 the landslide hazards in the forereservoir region of the Three Gorges Project on the
637 Yangtze River. Engineering Geology 59(1–2), 51-58
638 Xu, R.C., Zhou, J.J., 2010. Red bed and dam. Wuhan: China University of Geosciences
639 Press, second edition, 10-20 (in Chinese)
640 Yin, K.L., Wu, Y.P., 1998. Systematic research of one special paleo-landslide in the
641 Three-Gorges Reservoir. The Chinese Journal of Geological Hazard and Control, 9(S):
642 200-206 (in Chinese).
643 Yin, Y.P., Wang, H.D., Gao, Y.L., Li, X., 2010. Real-time monitoring and early warning of
644 landslides at relocated Wushan Town, the Gorges Resrvoir, China. Landslides 7(3),
645 339-349.

Captions:

Fig. 1. Location of the Three Gorges Reservoir in China.

Fig. 2. Curves of maximum accumulated displacement with time for 21 typical landslides in Jurassic red-strata in the Three Gorges Reservoir. (a) Maximum accumulated displacement is smaller than 100 mm; (b) maximum accumulated displacement is larger than 100 mm.

Fig. 3. Conceptual model for the slow movement of landslides in Jurassic red-strata in the Three Gorges Reservoir before their catastrophic failure. (a) Accumulated displacement versus time; (b) Displacement rate versus time.

Fig. 4. Xiangshanlu landslide (with a yellow asterisk mark), nearby Qianjiangping landslide, which occurred in the early morning on July 14, 2003 and caused 24 people died (Wang, et al., 2004; Liao, et al., 2005). (Image from Google Earth) (a):Location of the landslide in TGR; (b) details of landslide locations marked on Google Earth image.

Fig. 5. Xiangshanlu landslide. (a) Houses destroyed in the toe of the landslide; (b) sliding mass; (c) soils within the sliding zone; (d) thickness of the soils within the sliding zone; and (e) profile of the sliding mass.

Fig. 6. Indices of physical properties of soil sample from Xiangshanlu landslide (XSL sample). (a) Grain size distribution of sample XSL; (b) plasticity chart of XSL sample.

Fig. 7. Ring shear test on the XSL sample. (a) Undrained shear behavior with the normal stress of 98 kPa; (b) residual shear strengths at different normal stresses.

Fig. 8. Ring shear test on the XSL sample at different shear speeds under the normal stress of 196 kPa.

Fig. 9. Ring shear test on the XSL sample with the different consolidation duration under the normal stress of 196 kPa. (a) shear resistance vs. shear displacement; and (b) vertical displacement vs. shear displacement.

Fig. 10. Configuration in the test of changing the pore-water pressure of shear zone.

Fig. 11. Shear behaviour of the sample XSL in the test of changing the pore-water pressure of shear band. (a) Shear stress and pore-water pressure versus time; (b) effective normal stress path in the test.

Table 1. Basic physical properties index of the soils within the sliding zone of Xiangshanlu landslide

Physical properties index	ρ_d / g/cm^3	w_L / %	w_P / %	I_P	C_u	C_c
XSL	1.75	49.50	27.70	21.80	24.13	57.44

Note: XSL, short for the sample collected from the sliding zone of Xiangshanlu landslide; ρ_d: dry density; w_L: liquid limit; w_P: plastic limit; I_P: plastic index; C_u: uniformity coefficient; C_c: coefficient of curvature.

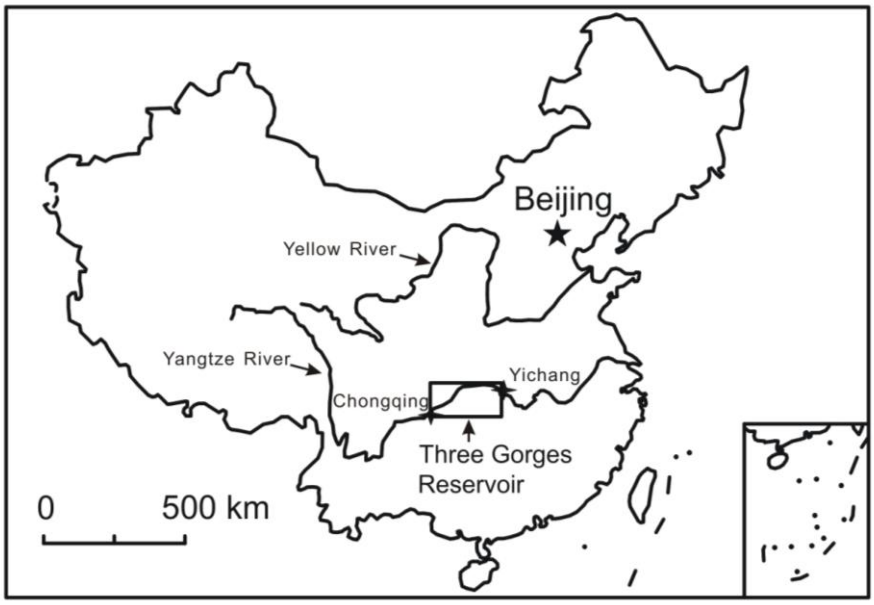

Fig. 1. Location of the Three Gorges Reservoir in China.

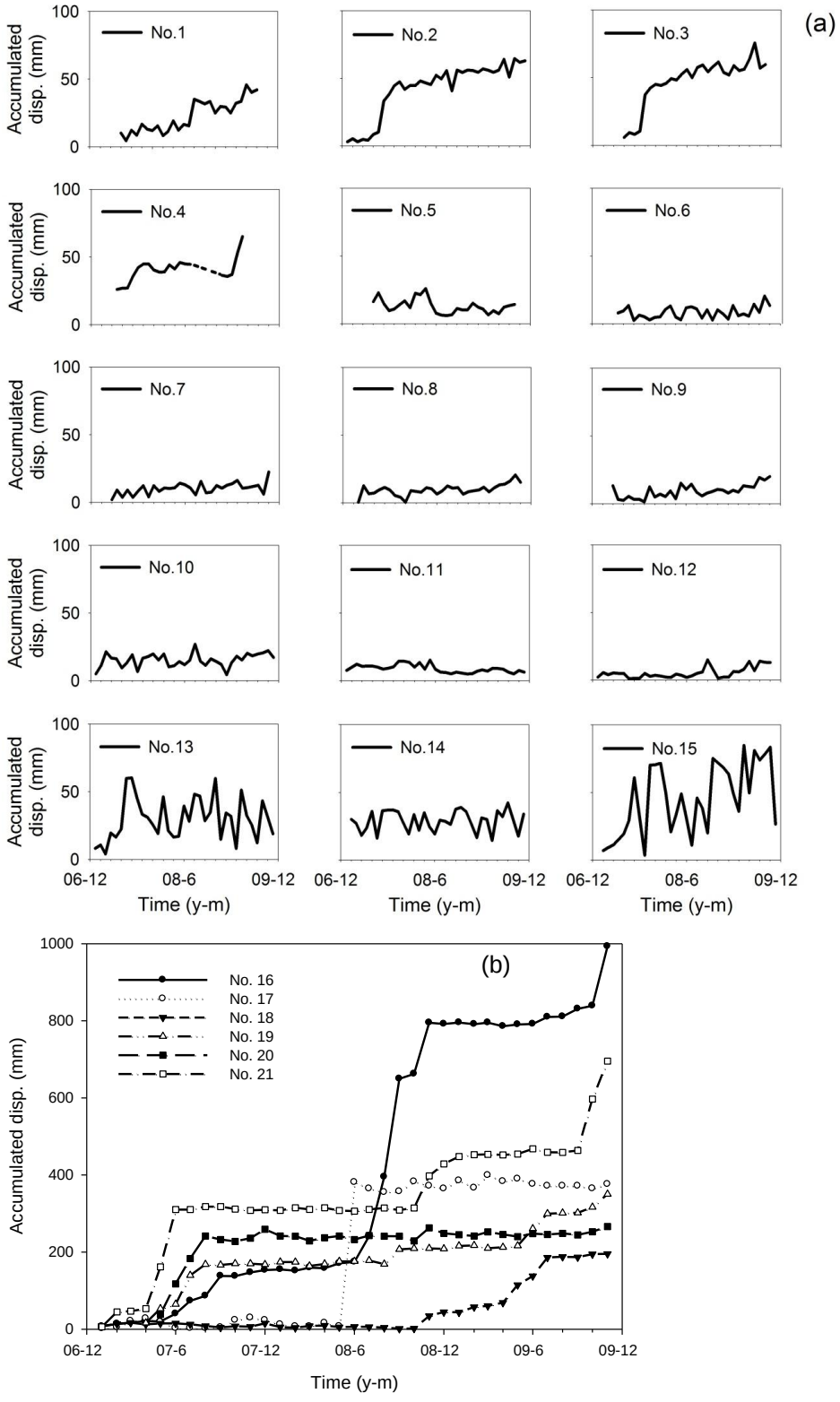

Fig. 2. Curves of maximum accumulated displacement with time for 21 typical landslides in Jurassic red-strata in the Three Gorges Reservoir. (a) Maximum accumulated displacement is smaller than 100 mm; (b) maximum accumulated displacement is larger than 100 mm.

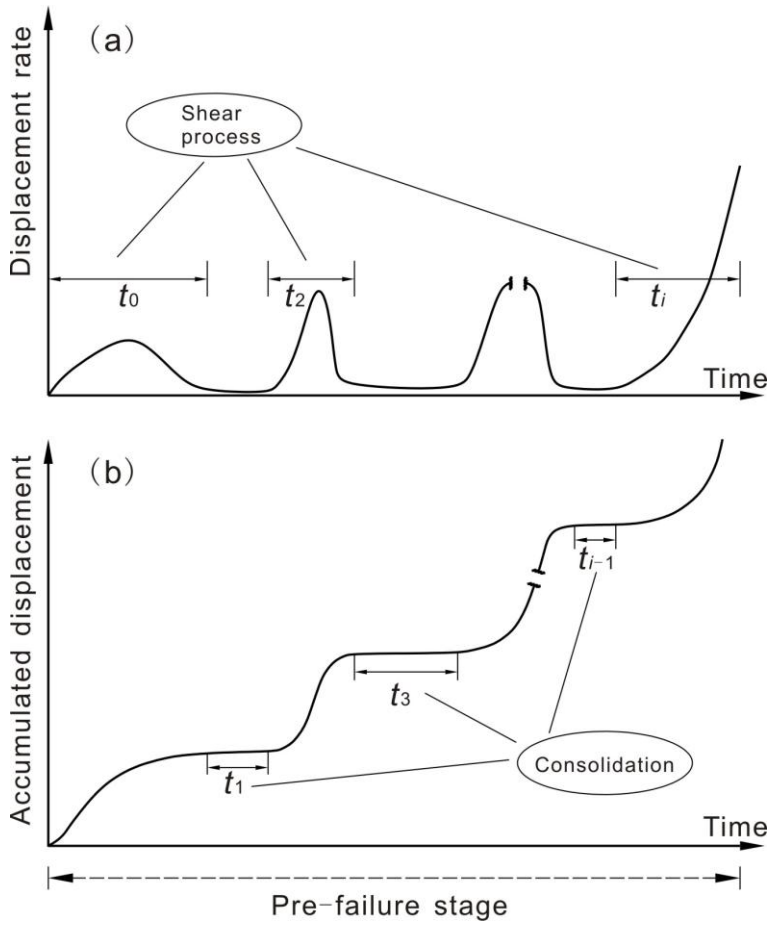

Fig. 3. Conceptual model for the slow movement of landslides in Jurassic red-strata in the Three Gorges Reservoir before their catastrophic failure. (a) Accumulated displacement versus time; (b) Displacement rate versus time.

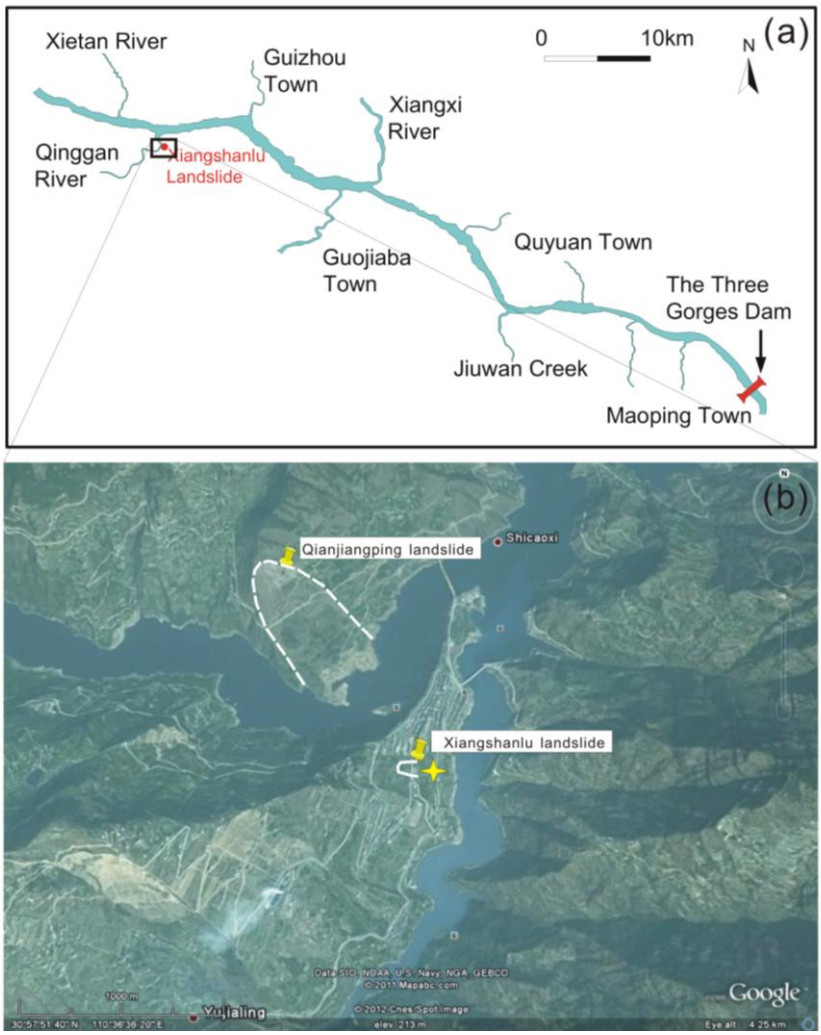

Fig. 4. Xiangshanlu landslide (with a yellow asterisk mark), nearby Qianjiangping landslide, which occurred in the early morning on July 14, 2003 and caused 24 people died (Wang, et al., 2004; Liao, et al., 2005). (Image from Google Earth) (a):Location of the landslide in TGR; (b) details of landslide locations marked on Google Earth image.

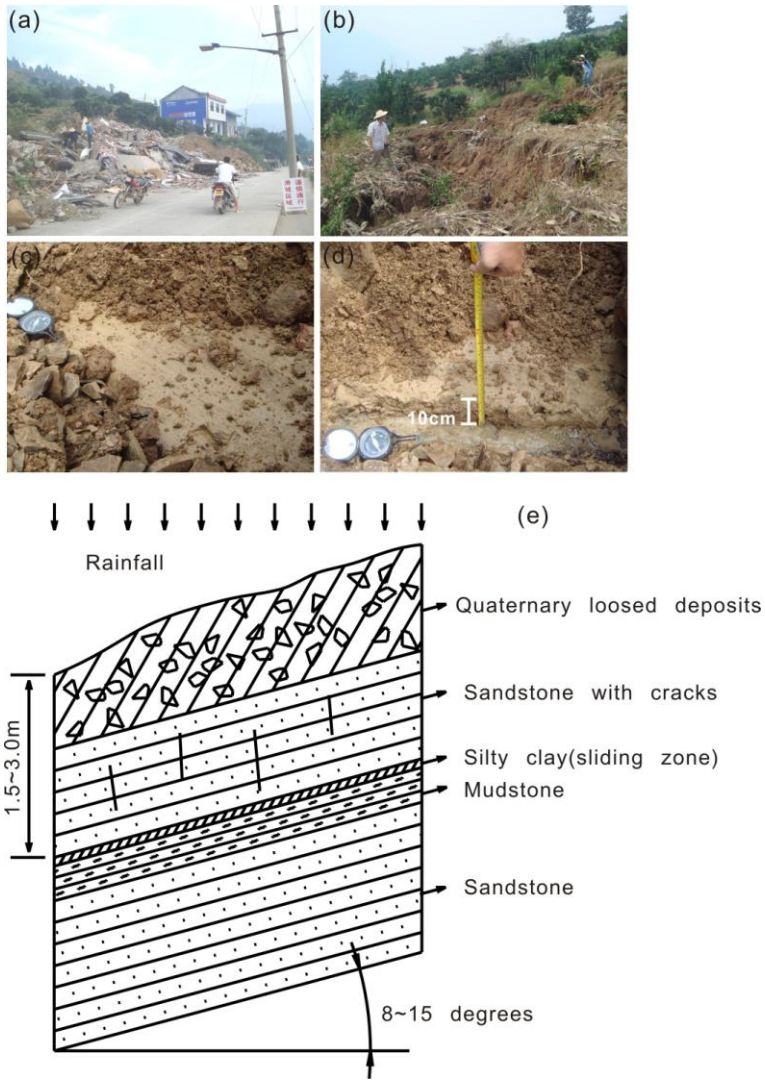

Fig. 5. Xiangshanlu landslide. (a) Houses destroyed in the toe of the landslide; (b) sliding mass; (c) soils within the sliding zone; (d) thickness of the soils within the sliding zone; and (e) profile of the sliding mass.

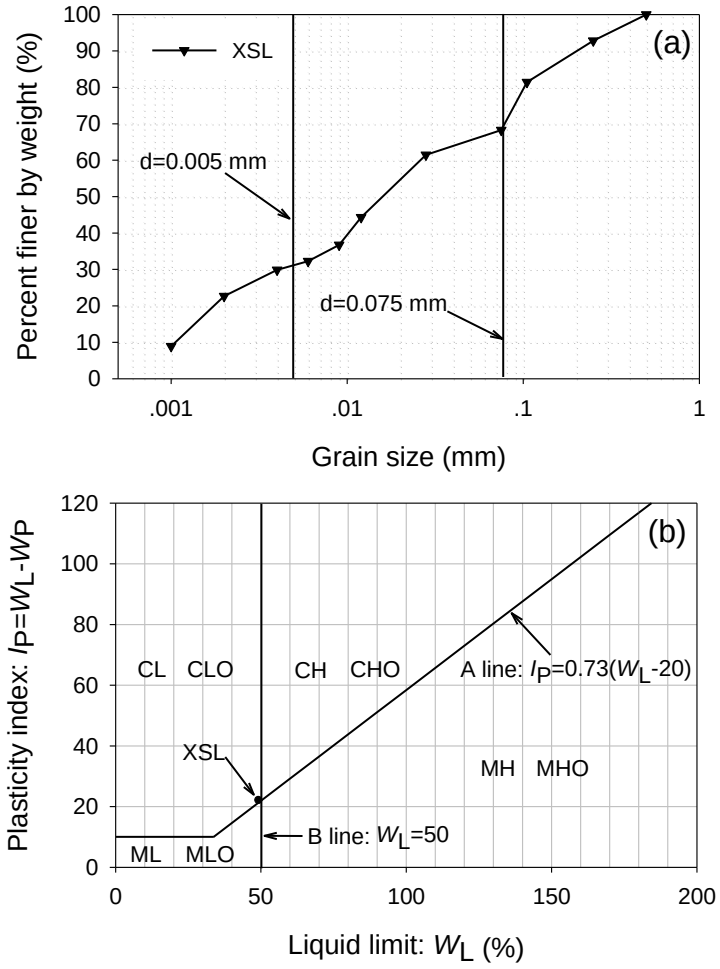

Fig. 6. Indices of physical properties of soil sample from Xiangshanlu landslide (XSL sample). (a) Grain size distribution of sample XSL; (b) plasticity chart of XSL sample.

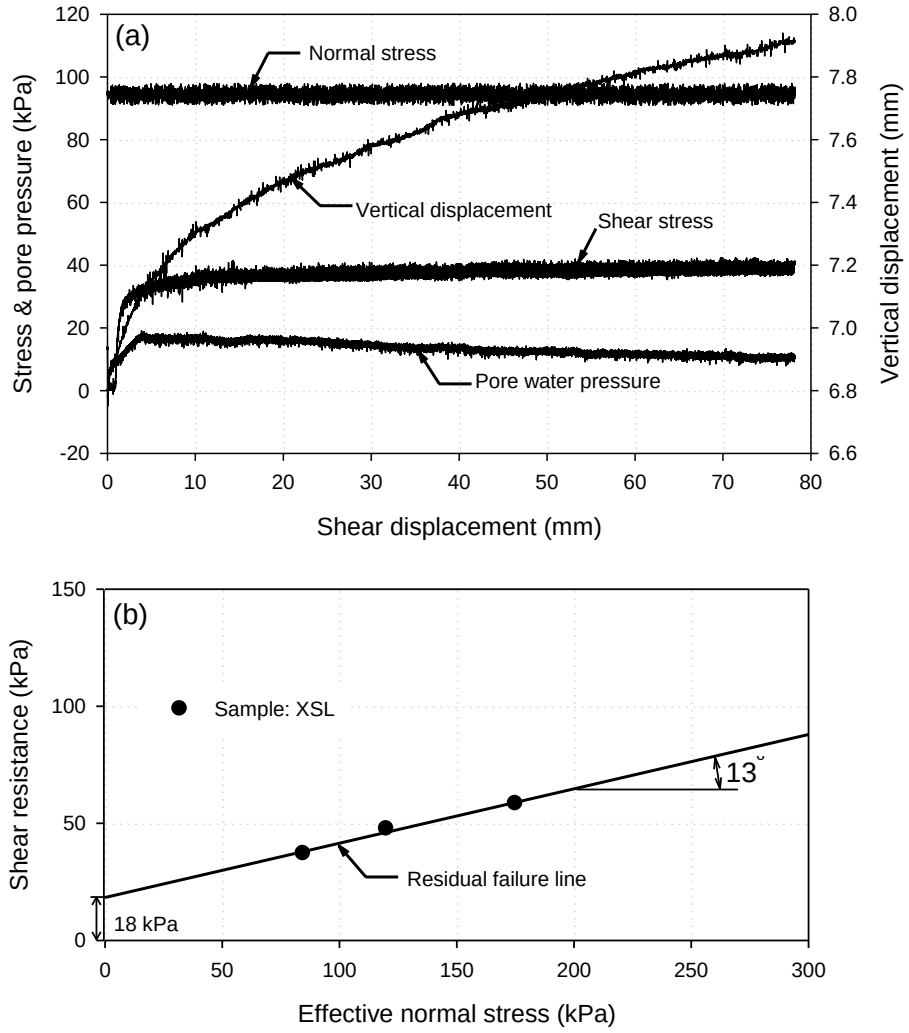

Fig. 7. Ring shear test on the XSL sample. (a) Undrained shear behavior with the normal stress of 98 kPa; (b) residual shear strengths at different normal stresses.

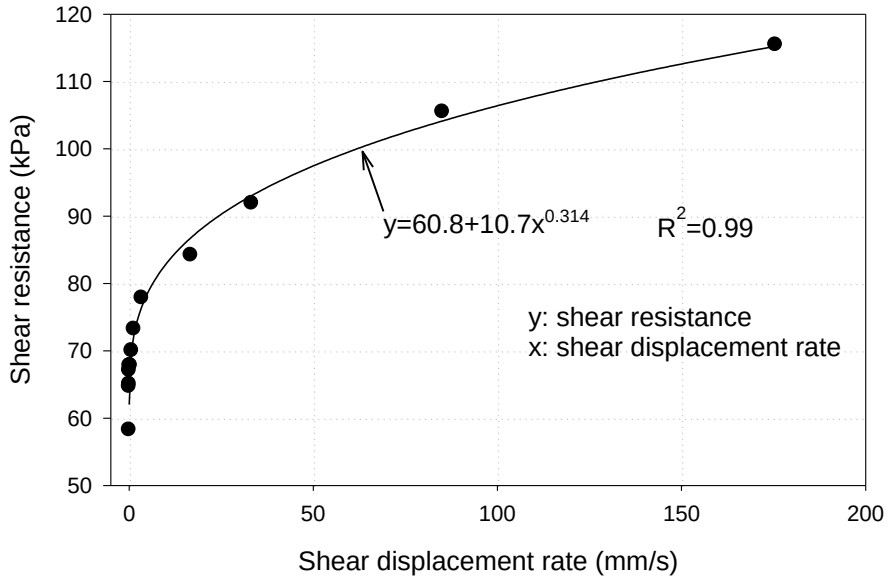

Fig. 8. Ring shear test on the XSL sample at different shear speeds under the normal stress of 196 kPa.

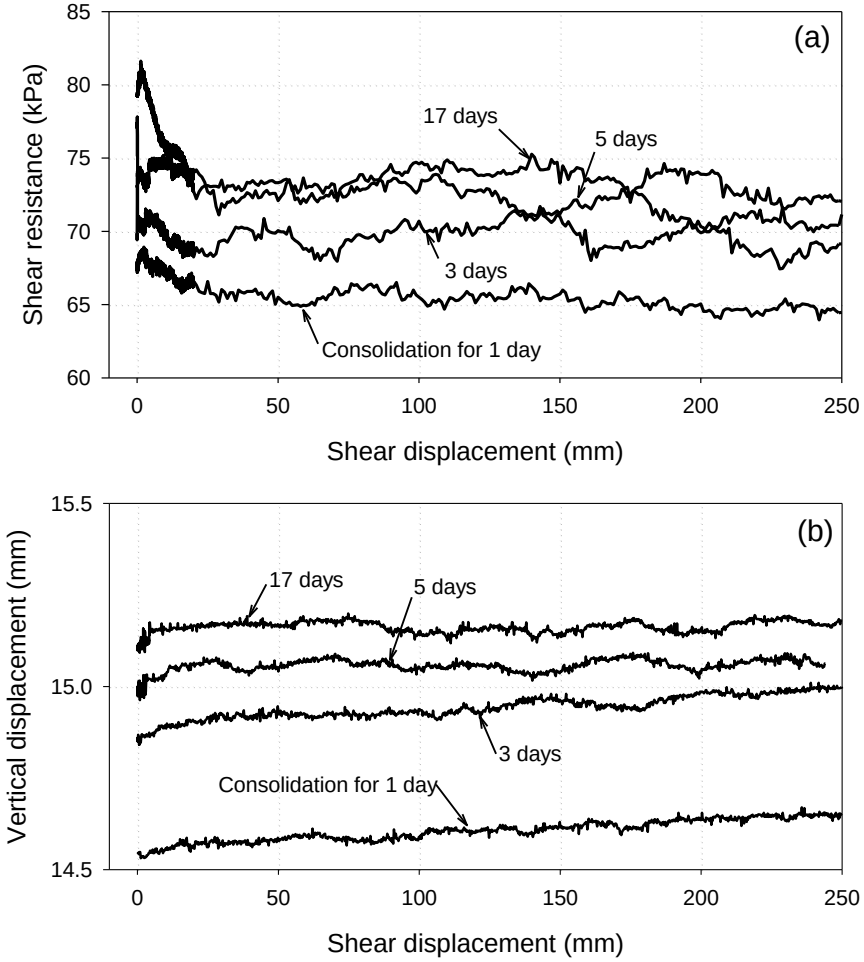

Fig. 9. Ring shear test on the XSL sample with the different consolidation duration under the normal stress of 196 kPa. (a) shear resistance vs. shear displacement; and (b) vertical displacement vs. shear displacement.

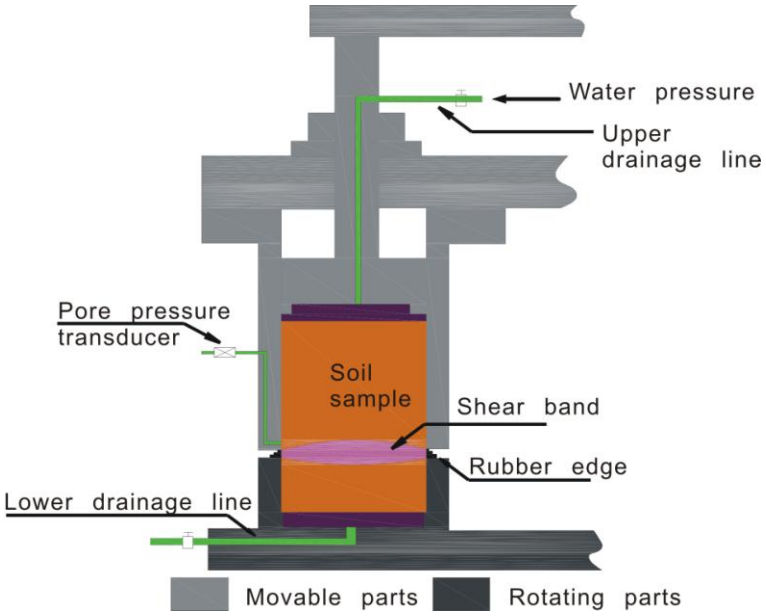

Fig. 10. Configuration in the test of changing the pore-water pressure of shear band.

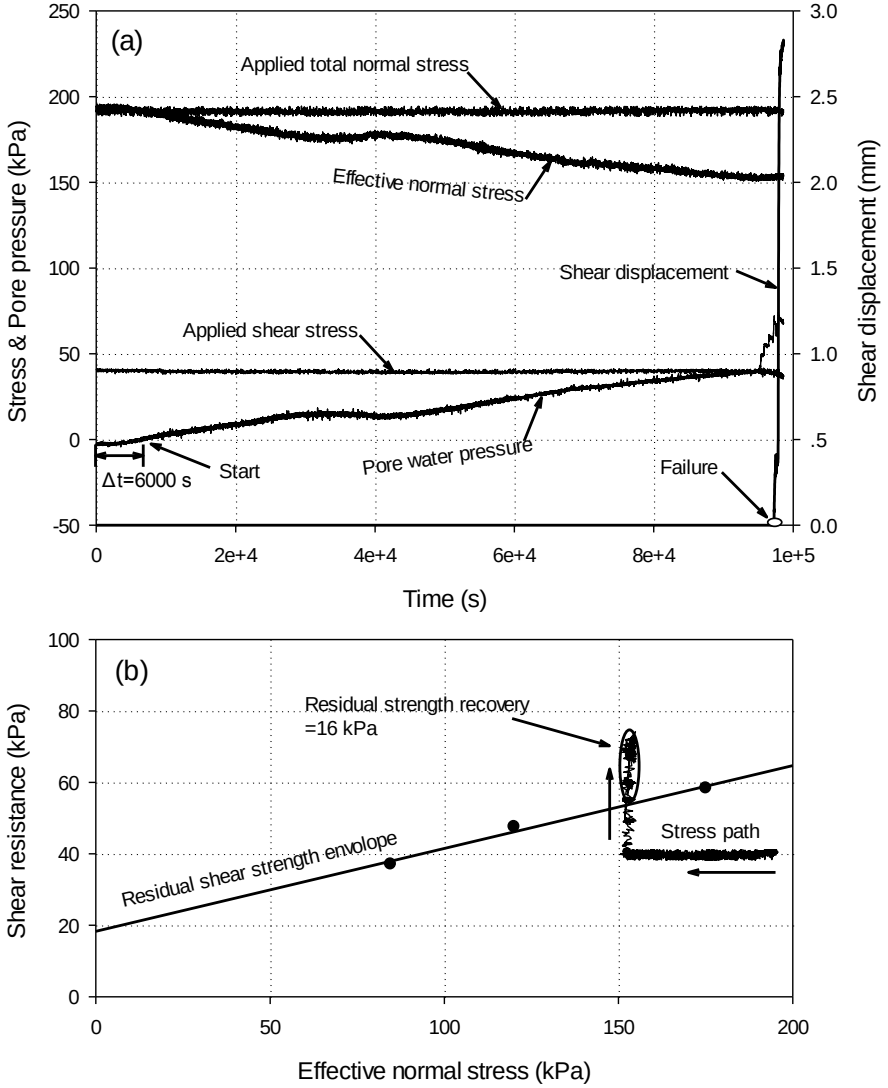

Fig. 11. Shear beheavoir of the sample XSL in the test of changing the pore-water pressure of shear band. (a) Shear stress and pore-water pressure versus time; (b) effective normal stress path in the test.